HAL open science

2-D Volume Integral Formulations for Nonlinear Magneto-Static Field Computation for Rotating Machines Pre-Design Considering Periodicities

Quentin Debray, Gérard Meunier, Olivier Chadebec, Jean-Louis Coulomb, Anthony Carpentier

To cite this version:

Quentin Debray, Gérard Meunier, Olivier Chadebec, Jean-Louis Coulomb, Anthony Carpentier. 2-D Volume Integral Formulations for Nonlinear Magneto-Static Field Computation for Rotating Machines Pre-Design Considering Periodicities. IEEE Transactions on Magnetics, 2018, 54 (3), pp.7001604. 10.1109/TMAG.2017.2752767 . hal-02278111

HAL Id: hal-02278111

https://hal.science/hal-02278111v1

Submitted on 14 Nov 2019

HAL is a multi-disciplinary open access archive for the deposit and dissemination of scientific research documents, whether they are published or not. The documents may come from teaching and research institutions in France or abroad, or from public or private research centers.

L'archive ouverte pluridisciplinaire **HAL**, est destinée au dépôt et à la diffusion de documents scientifiques de niveau recherche, publiés ou non, émanant des établissements d'enseignement et de recherche français ou étrangers, des laboratoires publics ou privés.

2D Volume Integral Formulations for Nonlinear Magneto-static Field Computation for Rotating Machines Pre-Design Considering Periodicities

Quentin Debray[1,2,3], Gerard Meunier[1,2], Olivier Chadebec[1,2], Jean-Louis Coulomb[1,2], Anthony Carpentier[3]
email : qdebray@altair.com

***Abstract*—This paper provides an alternative approach to the finite elements method of solving magneto-static field for an efficient pre-design of electrical rotating machines [2][3]. First, the 2D volume integral formulation will be presented. Second, this formulation will be extended to periodic systems. Comparisons to the finite elements methods will be carried out to conclude on the performances of the new method presented.**

I. INTRODUCTION

For a few years, Volume Integral Method (VIM) has been widely studied [6][1][4] and is know today as a good alternative to the Finite Elements Method (FEM) for solving magnetostatic problems in the presence of non-linear materials. While the FEM needs the geometry to be completely meshed, the VIM only requires the meshing of active materials. Moreover, while the FEM only takes into acount local approximated interactions between Degrees Of Freedom (DOF), VIM considers Green kernel type interaction. Those types of interactions allow to be as efficient as possible on a given mesh since the quality of the calculation of the interaction is very high. Nevertheless, analytical methods are necessary to correcly compute the integration of the Green kernel since they are singular. This allows the use of lighter meshes. While several VIM formulations have already been proposed in 3D [5][1][4] using different types of unknows (magnetization, scalar potential, magnetic field, etc...), 2D VIM have never been developed. Moreover VIM have been used in eletrical engine simulation. Since the 3D VIMs yield good results, we decided to implement them in 2D to test its efficiency in an electrical engine pre-design context. The switchover form 3D to 2D is far from being trivial since the Green kernels are different. Thus all the analytical integration are to be recalculated. This papers presents a 2D formulation based on the magnetic vector potential. We will first display the major equations leading to the non linear system to be solved and then apply this technique to electrical engine pre-design.

II. 2D VOLUME INTEGRAL METHOD

The Volume Integral Method (VIM) used in this paper is a vector potential formulation. It will be briefly presented in this document however the reader can refer to the full description of this method in 3D in [1]. The problem to be treated is presented in figure 1. The domain Ω is a surface domain

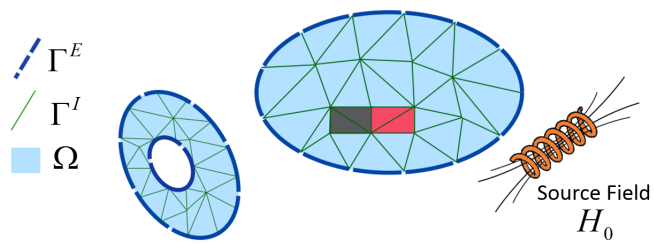

Fig. 1. Statement of the problem

representing the ferro-magnetic region including the magnets (described with red and black color on the figure 1). Domain Γ^E represents the set of facets on the outside of the domain Ω while Γ^I reprensents the internal facets Ω. We can thus define $\Gamma^T = \Gamma^I + \Gamma^E$. Induction vector $\mathbf{B}$ can be approximated by the Whitney facet elements [7] which yields the first order interpolation :

$$\mathbf{B} = \sum_{i=1}^{N_f} \mathbf{w}_{fi}\Phi_i \tag{1}$$

where Φ_i is the magnetic flux across the facet i. The constitutive equations of the magnetosatic $\mathbf{B} = \mu(\mathbf{B})\mathbf{H}$ and $\mathbf{H} + \nabla\varphi_{red} = \mathbf{H}_0$ lead to the equation :

$$\nu(\mathbf{B})\mathbf{B} + \nabla\varphi_{red} = \mathbf{H}_0 + \mathbf{H}_c \tag{2}$$

φ_{red} is the scalar reduced potential that can be expressed as displayed in equation (3) :

$$\varphi_{red} = \frac{1}{2\pi}\int_\Omega \mathbf{M}\cdot\nabla G \ \mathrm{d}\Omega \tag{3}$$

where $G(\mathbf{r})$ is the 2D Green kernel definied as $G(\mathbf{r}) = -\log(\|\mathbf{r}\|)$ and $\mathbf{M}$ is the magnetization of the material. $\mathbf{H}_0$ is the source term created by the coils. A Galerkin projection of this equation over the facet shape functions of the domain leads to :

$$\begin{aligned}\int_\Omega \mathbf{w}_i\nu(\mathbf{B})\mathbf{B}\mathrm{d}\Omega + \int_\Omega \mathbf{w}_i\cdot\nabla\varphi_{red}\mathrm{d}\Omega = \\ \int_\Omega \mathbf{w}_i\cdot(\mathbf{H}_0+\mathbf{H}_c)\mathrm{d}\Omega\end{aligned} \tag{4}$$

which conducts the matricial system :

$$\mathcal{R}^B\mathbf{\Phi} + \mathcal{I} = \mathcal{F}^B \tag{5}$$

[1]1Univ. Grenoble Alpes, G2Elab, F-38000 Grenoble, France
[2]CNRS, G2Elab, F-38000 Grenoble, France
[3]Altair Engineering, 15 chemin de Malacher, 38340 Meylan, France

where $\mathcal{R}$ is a finite element like matrix and $\mathcal{F}$ is the second hand :

$$\mathcal{R}_{ij}^B = \int_\Omega \mathbf{w}_i \cdot \nu(\mathbf{B})\mathbf{w}_j \mathrm{d}\Omega \tag{6}$$

$$\mathcal{F}_i^B = \int_\Omega \mathbf{w}_i \cdot (\mathbf{H}_0 + \mathbf{H}_c)\mathrm{d}\Omega \tag{7}$$

$$\mathcal{I}_i = \int_\Omega \mathbf{w}_i \cdot \nabla\varphi_{red}\mathrm{d}\Omega \tag{8}$$

$\mathcal{I}$ is the Green kernel-like interaction term. After the developments found in [1] the matricial system (5) is modified :

$$\begin{aligned} &\text{find } \mathbf{\Phi}_m \in \mathbb{R}^{N_{fi}} \text{ such as :} \\ &\mathcal{M}(\mathcal{R}^B + \mathcal{L}^B)\mathcal{M}^T\mathbf{\Phi}_m = \mathcal{M}(\mathcal{F}^B + \mathcal{G}^B) \end{aligned} \tag{9}$$

where matrix $\mathcal{M}$ is and independant loop matrix, $\mathbf{\Phi}_m$ is the loop flux defined as $\mathbf{\Phi}_m = \mathcal{M}\mathbf{\Phi}$ and N_{fi} is the size of the vector $\mathbf{\Phi}_m$. Matrices $\mathcal{L}^B$ and $\mathcal{G}^B$ are defined as :

$$\mathcal{L}_{ij}^B = \frac{1}{2\pi}\frac{\delta\nu_j}{l_i l_j}\int_{\Gamma_i^E}\int_{\Gamma_j^T} G(\mathbf{r})\ \mathrm{d}\Gamma_j^T\ \mathrm{d}\Gamma_i^E \tag{10}$$

$$\mathcal{G}_i^B = \frac{1}{2\pi}\frac{1}{l_i}\sum_{j=1}^{N_f}\int_{\Gamma_i^E}\int_{\Gamma_j^T} G(\mathbf{r})\delta H_{cnj}\ \mathrm{d}\Gamma_j^T\ \mathrm{d}\Gamma_i^E \tag{11}$$

where $\delta\nu_j$ is the reluctivity jump between the two elements sharing facet j, and δH_{cnj} is the normal residual magnetization jump between the two elements sharing facet j (which is not equal to zero unless facet j is at the border of a magnet). Scalar l_j represents the length of the facet j. One would notice that the $\mathcal{L}^B$ is not be integrated for every iterations of the Newton-Raphson solver in the presence of non linear materials. The matrix only have to be uptated with the vector of reluctivity jumps. This saves a considerable amount of time during the non-linear solving process.

A variation of this loop flux formulation is an $\mathbf{A}$ formulation where $\mathbf{A}$ is interpolated on edge elements :

$$\mathbf{A} = \sum_{i=1}^{N_a}\mathbf{w}_{ai}A_i \tag{12}$$

where $\mathbf{w}_{ai}$ is the shape function of the edge number i. Indeed, the facet flux can be expressed as $\Phi = [\nabla\times]\mathbf{A}$ where $[\nabla\times]$ is the discrete version of $\nabla\times$ differential operator. This discrete version corresponds to the incidence matrix facet$\rightarrow$ edge. This incidence matrix presents the same properies as an idependent loops matrix [1]. Thus an $\mathbf{A}$ formulation is obtained similarly to (9) :

$$\begin{aligned} &\text{find } \mathbf{A} \in \mathbb{R}^{N_a} \text{ such as :} \\ &[\nabla\times]^T(\mathcal{R}^B + \mathcal{L}^B)[\nabla\times]\mathbf{A} = [\nabla\times]^T(\mathcal{F}^B + \mathcal{G}^B) \end{aligned} \tag{13}$$

where all the matrices are defined above and N_a is the number of edges of the domain Ω. One of the key points of this method is to accuratly calculate the terms :

$$e = \int_{\Gamma_i^E}\int_{\Gamma_j^T} G(\mathbf{r})\ \mathrm{d}\Gamma_j^T\ \mathrm{d}\Gamma_i^E \tag{14}$$

in (10) and (11). A semi-analytic approach is used to discretise this expression to :

$$e \simeq \sum_{k=1}^{N_G}\int_{\Gamma_i^E}\log(\frac{1}{r_k})\ \mathrm{d}\Gamma_i\mathbf{w}_k^G \tag{15}$$

where $\mathbf{w}_k^G$ is the Gauss weight of gauss point k, N_G is the number of Gauss points used to discretize Γ_j^T and r_k is the distance between Gauss point k of Γ_j^T and the integration point along Γ_i^E. Analytical formulas exist [8] to calculate the exact value of :

$$\int_{\Gamma_i^E}\log(\frac{1}{r_k})\ \mathrm{d}\Gamma_i \tag{16}$$

This approach allows us to compute integrals (10) and (11) with a high level of precision and thus attain fairly accurate results even with a very coarse mesh.

III. VALIDATION

The formulation has been tested by calculating the field in the air gap of a permanent magnet rotating machine (PMRM). Since this machine is periodic, only one quarter is shown in figure 2. The radial magnets are opposed in direction (the one on the far right is oriented towards the outside while the other one is oriented in the opposite direction). The coils of PMRM are powered with a 1000A tree-phase current. The magnetic field in the air gap of the machine is computed with the relation (17) where $\mathbf{M}$ is obtained via $\mathbf{M} = (\nu_0 - \nu(\mathbf{B}))\nabla\times\mathbf{A}$. The results obtained with the VIM are compared to a converged finite element solution and plotted in figure 4.

$$\mathbf{B} = -\frac{\mu_0}{2\pi}\nabla\int_\Omega \mathbf{M}\cdot\nabla G(r)\mathrm{d}\Omega + \mu_0\mathbf{H}_0 \tag{17}$$

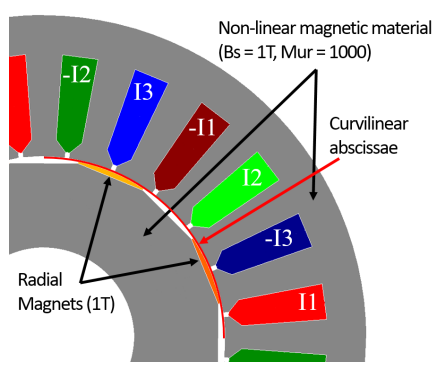

Fig. 2. Description of test case

For this test case, we used a mesh quite poor in quality (900 unknowns for the full PMRM) illustrated figure 3 that nevertheless gave us a mean error of 2.5% with a maximum error of 10%. We can conclude from this test that even with few DOF, the VIM is efficient for difficult cases of magneto static field computation.

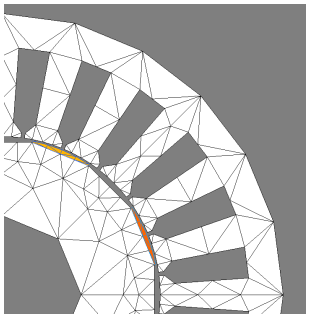

Fig. 3. Mesh used for the validation of the formulation

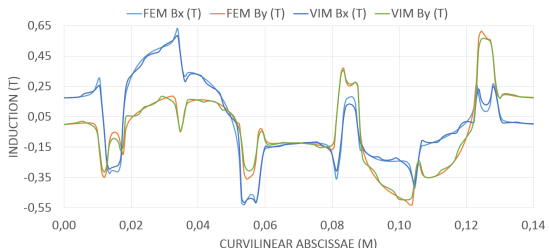

Fig. 4. induction profile in the airgap of the machine (red line displayed figure 2)

IV. PERIODICITY ADAPTED VIM

Since most PMRM are periodic one would want to take advantage of this characteristic in order to decrease the number of unknowns and thus the computation time. An adapted formulation for the VIM is described below. In order to to properly describe this adapted formulation, one must firstly define several domains : indeed, in contrast to the FEM in which the periodicities are taken care of with boudary conditions on the periodic domain, the VIM and its Green kernel interaction terms impose to use the whole mesh for the integration of the terms $\mathcal{L}^B$ and $\mathcal{G}^B$. Thus we define a "real" domain, for which Ω^R, Γ^{ER} and Γ^{TR} refer. The construction of the linear system will concern the DOF contained in Ω^R. Nevertheless, contribution from "ghost" domains will be taken into account. The "ghost" domain are indiced "Fk". Letter "k" corresponds to the number of ghost domains since there can be several. A summary of those notations is found figure 5 which is a simplified description of a $\frac{\pi}{2}$ anti-periodic PMRM.

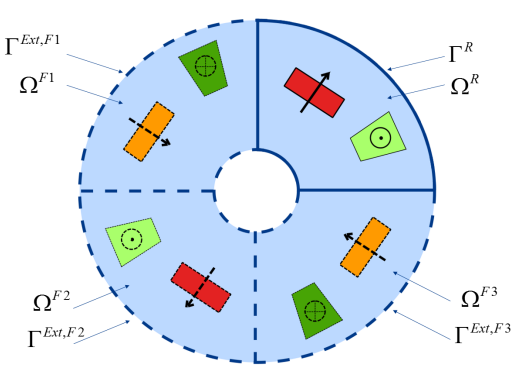

Fig. 5. notations for the periodicity adapted formulation

The contribution of the ghost domains to the matrices $\mathcal{L}^B$ and $\mathcal{G}^B$ yields a new equation system :

$$\begin{aligned} &\text{find } \mathbf{A} \in \mathbb{R}^{N_a^{per}} \text{ such as :} \\ &[\nabla\times]^T \left(\mathcal{R}^B_{per} + \mathcal{L}^B_{per}\right)[\nabla\times]\,\mathbf{A} = [\nabla\times]^T \left(\mathcal{F}^B_{per} + \mathcal{G}^B_{per}\right) \end{aligned} \tag{18}$$

where

$$\begin{aligned} (\mathcal{R}^B_{per})_{ij} &= \int_{\Omega^R} \nabla\times\mathbf{w}_i \cdot \nu(\mathbf{B})\nabla\times\mathbf{w}_j \mathrm{d}\Omega^R \\ (\mathcal{L}^B_{per})_{ij} &= \frac{1}{2\pi}\frac{\delta\nu_j^R}{l_i^E l_j^T}\int_{\Gamma_i^{ER}}\int_{\Gamma_j^{TR}} G(\mathbf{r})\mathrm{d}\Gamma_j^{TR}\mathrm{d}\Gamma_i^{ER} \\ &\quad + \frac{1}{2\pi}\frac{\delta\nu_j^{Fk}}{l_i^E l_j^T}\sum_{k=1}^{N_F}\int_{\Gamma_i^{EFk}}\int_{\Gamma_j^{TR}} G(\mathbf{r})\mathrm{d}\Gamma_j^{TR}\mathrm{d}\Gamma_i^{EFk} \end{aligned} \tag{19}$$

and

$$\begin{aligned} (\mathcal{F}^B_{per})_i &= \int_{\Omega^R} \nabla\times\mathbf{w}_i\cdot(\mathbf{H}_c + \mathbf{H}_0^R)\mathrm{d}\Omega^R \\ &\quad + \sum_{k=1}^{N_F}\int_{\Omega^R}\nabla\times\mathbf{w}_i\cdot\mathbf{H}_0^{Fk}\mathrm{d}\Omega^R \\ (\mathcal{G}^B_{per})_i &= \frac{1}{2\pi l_i^E}\int_{\Gamma_i^{ER}}\left\{\sum_{j=1}^{N_a^{per}}\int_{\Gamma_j^{TR}}\delta H_{cn}^R G(\mathbf{r})\mathrm{d}\Gamma_j^{TR}\right\}\mathrm{d}\Gamma_i^{ER} \\ &+ \frac{1}{2\pi l_i^E}\sum_{k=1}^{N_F}\int_{\Gamma_i^{EFk}}\left\{\sum_{j=1}^{N_a^{per}}\int_{\Gamma_j^{TR}}\delta H_{cn}^{Fk} G(\mathbf{r})\mathrm{d}\Gamma_j^{TR}\right\}\mathrm{d}\Gamma_i^{EFk} \end{aligned} \tag{20}$$

One can notice that this new system requires the values of $\delta\nu^{Fk}$ and δH_{cn}^{Fk} but since those values are scalar it is possible to express them from $\delta\nu^R$ and δH_{cn}^R. If the ghost domain is periodic,$\delta\nu^{Fk} = \delta\nu^R$ and if the ghost domain is anti-periodic, $\delta\nu^{Fk} = -\delta\nu^R$. It is similar for δH_{cn}^{Fk}. Thanks to this periodic formulation, the real domain becomes $1/8^{th}$ of the full PMRM. It is possible to decrease the number of unknowns again since one eighth of the domain presents an axial symmetry if there is no current in the coils. Neverthless, we didn't consider this in the study since the symmetry is easily lost (non symmetrical coils, movement of the rotor).

V. COMPUTATION PERFORMANCES

We tested this periodic formulation on the test case described figure 2 in short circuit. We used two qualities of mesh, a coarse one with 900 DOF in the full geometry and one more refined with 3600 DOF in the full geomtry. The computation time for several exploitation of the geometry are summed up in the table I. For each cell of the table, the first value is the time required to do the calculation with the fine mesh, and the second number refers to the coarse mesh. Considering the small number of unknowns, we compared two techniques to solve the linear systems (iterative solver GMRES and direct solver via LU decomposition).

TABLE I
COMPARISON OF COMPUTATION TIME FOR PERDIODIC AND ANTI-PERIODIC DOMAIN AND DIFFERENT SOLVERS

	Linear system construction	One iteration of NR solver	Total computation time
Full geometry (GMRES)	3.75s/0.41s	2.02s/0.40s	33.78s/5.16s
Periodic Domain (GMRES)	0.94s/0.12s	0.53s/0.081s	8.22s/1.37s
Periodic Domain (LU)	0.85s/0.29s	0.46s/0.044s	7.55s/0.89s
Anti-periodic Domain (GMRES)	0.58s/0.19s	0.27/0.081s	4.27s/1.12s
Anti-periodic Domain (LU)	0.72s/0.16s	0.13s/0.023s	2.80s/0.45s

We can see that the less unknowns in the system, the more the LU solver is efficient compared to the GMRES solver. For the system with less than 900 DOF, the LU solver is then chosen. Since the symetric & anti-periodic case is rarely useful, we will consider the computation time of the $1/8^{th}$ of the domain with the LU solver as main result of this study. In short circuit, the mean error of the induction in the airgap drops to 1.5% with 125 DOF. This perfomance has to be compared to

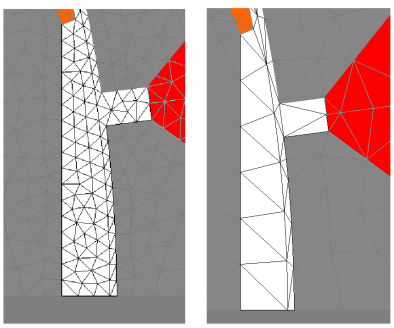

Fig. 6. two qualities of mesh for the FEM method. Good quality on the left (A) and bad quality on the right (B)

the FEM : the necessity to mesh the air (thus the airgap) with the FEM makes it impossible to drasticaly decrease the number of DOF an consequently the computation time. The test case displayed in figure 2 has been solved with the FEM solver embeded in the Flux software. The minimal number of DOF is constrained by the thinness of the airgap. It is not possible to decrease the number of elements in the airgap while keeping a good form factor for the elements. This is illustrated in figure 6. We tested the FEM method with those two meshes. While mesh (A) - 5000 DOF - yields good results (0.5% mean error) for the induction in the air gap, it takes the software roughly 4.01 seconds to compute the solution. 750 DOF are necessary to reach this level of precision with the periodic VIM. The mesh (B) has less DOF, around 3000, and yields less accurate results (2% mean error) in 3.72s. A summary of those results can be found in table II.

We can see that while the FEM is very well-suited for obtaining precise results (the sparsity of the linear system

TABLE II
COMPUTATION TIME AND PRECISION FOR METHODS FEM AND PERIODIC VIM

	FEM 5000 DOF	FEM 3000 DOF	P-VIM 125 DOF	P-VIM 750 DOF
Computation time	4.1s	3.7s	0.45s	4.6s
Mean error	0.55%	2.04%	1.5%	0.51%

to solve makes it easier to increase the number of DOF to a high level), it is poorly effective in terms of computation time for a pre-design objective. In contrast, the VIM - in addition to being as precise as the FEM for normaly meshed problems [1][5][4], last column of table II) - is very efficient for pre-design needs when the quality of the mesh is strongly degraded. Moreover, it is very to manage movement with the VIM since we just need to move the nodes of the moving part of the geometry. Indeed, the air is not meshed with this method and thus has not to be remeshed.

VI. CONCLUSIONS

An original 2D integral formulation has been presented and enhanced to take into account periodical systems. This method shows great promise for rotating machines pre-design since it yields fairly good results for a very limited amount of computation time and has a broad field of application (no hypotheses were made on the geometry nor the materials). This work has to be deepend to implement adapted post processing techniques. Two important post-processing would be the calculation of the torque on the rotor and the magnetic flux through the coils.

REFERENCES

[1] V. Le-Van, G. Meunier, O. Chadebec and J. M. Guichon, "A Volume Integral Formulation Based on Facet Elements for Nonlinear Magnetostatic Problems," in IEEE Transactions on Magnetics, vol. 51, no. 7, pp. 1-6, July 2015

[2] A. O. Di Tommaso, F. Genduso and R. Miceli, A novel improved matlab-based software for the electric and magnetic analysis and design of rotating electrical machines, 2015 Tenth International Conference on Ecological Vehicles and Renewable Energies (EVER), Monte Carlo, 2015, pp. 1-7.

[3] Juha Pythnen, Tapani Jokinen, Valria Hrabovcova, Design of Rotating Electrical Machines, Wiley Editions

[4] A. Carpentier, O. Chadebec, N. Galopin, G. Meunier and B. Bannwarth, "Resolution of Nonlinear Magnetostatic Problems With a Volume Integral Method Using the Magnetic Scalar Potential," in IEEE Transactions on Magnetics, vol. 49, no. 5, pp. 1685-1688, May 2013

[5] V. Le-Van, G. Meunier, O. Chadebec and J. M. Guichon, "A Magnetic Vector Potential Volume Integral Formulation for Nonlinear Magnetostatic Problems," in IEEE Transactions on Magnetics, vol. 52, no. 3, pp. 1-4, March 2016

[6] G. Meunier, O. Chadebec and J. M. Guichon, "A Magnetic FluxElectric Current Volume Integral Formulation Based on Facet Elements for Solving Electromagnetic Problems," in IEEE Transactions on Magnetics, vol. 51, no. 3, pp. 1-4, March 2015

[7] A. M. Vishnevsky, A. G. Kalimov and A. A. Lapovok, "Modeling magnetization using Whitney facet elements," in IEEE Transactions on Magnetics, vol. 38, no. 2, pp. 489-492, Mar 2002

[8] Emile Durand, "Magnetostatique - volume 1", 1968